# Plasmonic antiresonance through subwavelength hole arrays

**Daniel Maystre,* Anne-Laure Fehrembach, and Evgueni Popov**

*Institut Fresnel, UMR6133, Aix-Marseille Université, CNRS, Domaine Universitaire de Saint Jérôme, 13397, Marseille Cedex 20, France*
**Corresponding author: daniel.maystre@fresnel.fr*

Received October 27, 2010; accepted December 11, 2010;
posted January 10, 2011 (Doc. ID 137057); published February 17, 2011

It has been shown both experimentally and numerically that the phenomenon of extraordinary transmission through subwavelength hole arrays is generally associated with a drop in transmission located very close to it. Paradoxically, this antiresonant drop occurs at the wavelength that, at first glance, should provoke a resonant excitation of a surface plasmon propagating along the metallic surface of the screen. The present paper gives a theoretical demonstration of this phenomenon, which dispels the paradox. Our theory is supported by numerical calculations. 

*OCIS codes:* 050.6624, 050.0050, 260.2110, 050.1950.

## 1. INTRODUCTION

The phenomenon of extraordinary transmission of light through hole arrays has been widely analyzed in recent years, from both experimental data and theoretical results [1–25]. It is in general acknowledged that the resonant excitation of surface plasmons plays a key role in this surprising transmission phenomenon. Many papers have pointed out a very paradoxical result. Indeed, it turns out that a transmission drop occurs in the vicinity of the extraordinary transmission. The big paradox is that the wavelength that provokes this drop is precisely that for which a resonant excitation of a surface plasmon propagating along the metallic screen should arise. The aim of this paper is to give a theoretical demonstration of this phenomenon and to analyze numerically its limits.

Our demonstration of the existence of a drop is based on an assumption: the transverse width of the holes must be much smaller than both the wavelength of the light and the array period, but numerical results show that, in fact, width of holes of the order of half a period or half a wavelength are acceptable. Two cases are studied successively, according to whether the metallic screen is made of a perfectly conducting material or a real metal in the visible region. For each of them, we deal with one-dimensional (1D) (lamellar gratings) and two-dimensional (2D) (inductive grids) hole arrays.

In outline, the theory shows that the field in the hole array includes two parts: the field generated by a reflection on the flat, nonperforated screen and a field composed of two nonresonant (i.e., without resonantly enhanced amplitudes) surface waves propagating in opposite directions on the surface of the screen. This pair of surface waves is generated by the incident field at a wavelength corresponding to the excitation of surface plasmons on a flat, nonperforated screen. This result gives the explanation of the apparent paradox: the actual resonance phenomenon that provokes the phenomenon of extraordinary transmission occurs at the wavelength for which the actual surface plasmons of the perforated screen are excited, and thus it depends on both the shape of the holes and the optical index of the metal. On the other hand, the wavelength for which the drop occurs depends on the optical indices of the metal and dielectric only. When the size of the holes tends to zero, these two wavelengths tend to each other, and thus the drop and the extraordinary transmission annihilate each other.

It is worth noting that the demonstration of the existence of a drop extends to nonperiodic perforated structures, especially to the case of a single hole, but the present paper does not provide any numerical data for such structures, and thus no conclusion can be drawn.

## 2. PROBLEM AND NOTATIONS

The pair extraordinary transmission–transmission drop is evidenced by experimental measurements published by Genet *et al.* [26]. The experimental transmission curve is given in Fig. 1. A gold inductive grid made of a gold screen perforated by circular holes is illuminated in normal incidence by a plane wave. The smooth curve has been obtained by a free adjustment of parameters in a formula proposed by Fano. The arrow shows the wavelength corresponding to the excitation of surface plasmons on the upper interface of the screen by the $(1,0)$ order of the grating. Let us recall that the excitation of a surface plasmon by a 2D grating can be achieved by adjusting the propagation constant of an evanescent order generated by the grating to the propagation constant of the surface plasmon. Using the propagation constant of the surface plasmon propagating on a flat metallic surface and the grating formula, it is easy to deduce that in the experimental measurements shown in Fig. 1, the excitation occurs when the wavelength $\lambda$ in vacuum is related to the period $d$ of the grating by [27]

$$\lambda = \mathrm{Re}\left\{\frac{d\nu_M}{p\sqrt{1+\nu_M^2}}\right\}, \tag{1}$$

with the optical index of gold, $\nu_M$, the order exciting the surface plasmon here being either $(p,0)$ or $(0,p)$, depending on the

 

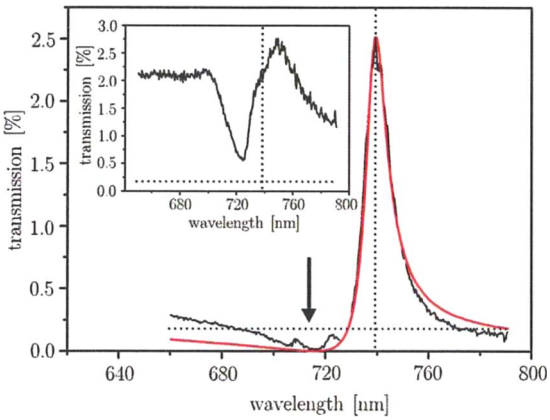


Fig. 1. (Color online) Experimental transmission spectrum of a gold film of thickness 200 nm with periods $d = d' = 700$ nm, the radius of the holes being equal to 70 nm. The smooth curve shows a theoretical curve obtained by adjusting freely the parameters in a formula proposed by Fano. The arrow shows the location of the drop given by Eq. (1). The inset shows the experimental transmission spectrum for the same array, but in a film 100 nm thick. Reprinted from Ref. [26], p. 335, with permission from Elsevier.

polarization of the incident wave (the direction of propagation of the surface plasmon being orthogonal to the direction of the incident magnetic field). The arrow in Fig. 1 corresponds to $p = 1$.

It is quite surprising to note that the wavelength that should excite a surface plasmon resonance in fact provokes a drop in transmission, the extraordinary transmission being shifted to a slightly larger wavelength. The explanation of this paradox will be given in this paper but, to this point, it should be noted that the constant of propagation of a surface plasmon on a grating differs from that on a flat surface, which can explain the shift of the resonance wavelength to the right. On the other hand, the existence of a drop in transmission at a wavelength given by Eq. (1) is quite puzzling. A demonstration of this phenomenon is given in the following, but it must be noted that, according to Eq. (1), the location of the drop should not depend on the radius of the holes. In order to verify this conjecture, in Fig. 2 we have drawn theoretical curves obtained by calculating the transmission of the inductive grid used by Genet *et al.* [26], but for various radii of holes.

In this paper, all calculations on metallic gratings with finite conductivity have been performed using a rigorous numerical code based on the Fourier modal method. The $S$-matrix propagation algorithm [28] and the correct factorization rules for the product of discontinuous functions are used to accelerate the convergence. Li's method [29] for 1D gratings, and the normal vector method by Popov and Nevière [30] for 2D gratings with circular holes, are applied. However, the convergence remains slow for gratings composed with an alternation of materials with real positive and real negative permittivity, a case in which the factorization rules enounced by Li are not available [31]. Nevertheless, the accuracy of the result is satisfactory with $(2 * 30 + 1)$ Fourier components, except for some configurations.

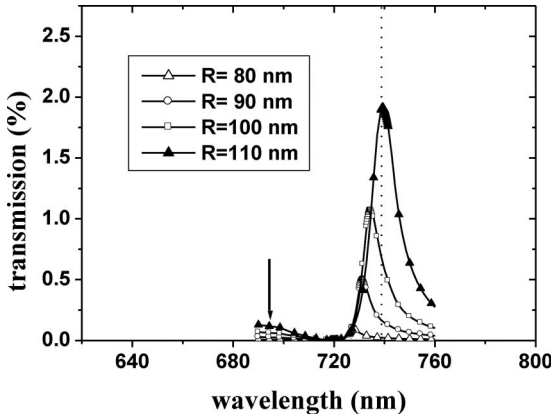


Fig. 2. Calculated transmission of the inductive grid corresponding to Fig. 1, for various values of the radius of the holes.

The calculations fully confirm the existence of an antiresonance at a wavelength slightly smaller than the wavelength of the extraordinary transmission. The curves are qualitatively similar to that shown in Fig. 1. However, the quantitative agreement on both the height and the location of the peak is obtained not for a radius of 70 nm, but for one of 110 nm. The explanation of this discrepancy could be found in a lack of precision on the actual radius and shape of the holes in the grating used by Genet *et al.* [26]

The vital conclusion to be drawn from Fig. 2 is that, in contrast with the location of the extraordinary transmission that is shifted to the right as the radius is increased, due to the shift of the actual surface plasmon of the perforated screen, the location of the antiresonance is independent of the radius of the holes and is given by Eq. (1).

The aim of the following is to provide a theoretical explanation to this apparently paradoxical result: an antiresonance is obtained when, at the first glance, a surface plasmon should be excited.

The grating is represented in Fig. 3. A metallic screen of width $h$ parallel to the $xz$ plane of a cartesian system of coordinates is perforated by holes parallel to the $y$ axis. These holes are located in parallel strips (called perforated strips in the following) of width $t$ (light gray regions at the left-hand side of Fig. 3) periodically spaced along the $x$ axis, with period $d$. The origin of the system of coordinates is located on the top of the screen, on the symmetry axis of one perforated strip. Figure 3(a) shows an inductive grid with circular holes of radius $R = t/2$ periodically located on the $x$ and $z$ axes, and Fig. 3(b) shows a lamellar grating, but the properties demonstrated in the paper can apply to many other cases. For example, the holes in each perforated strip can be arbitrarily

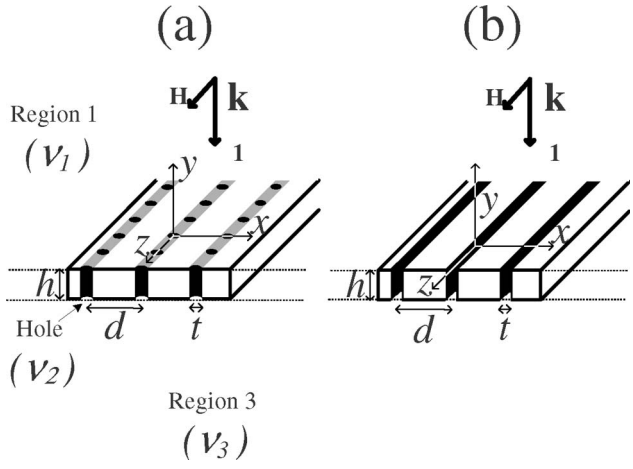


Fig. 3. Perforated metallic screen, scheme and notations. (a) Inductive grid, (b) lamellar grating.

located on the $z$ axis and are possibly finite in number. Our demonstrations include the case where the number of perforated strips is finite, but they always must be separated by multiples of $d$ on the $x$ axis, except, of course, in the case of a unique hole in the screen, which is also included. The regions 1 and 3 above and below the screen contain lossless dielectric materials of optical indices $\nu_1$ and $\nu_3$, respectively. The holes (region 2) are filled with a lossless dielectric of index $\nu_2$. The interfaces between the metallic regions and regions 1, 2, and 3 are denoted by $\Gamma_{M1}$, $\Gamma_{M2}$, and $\Gamma_{M3}$ while $\Gamma_{H1}$ and $\Gamma_{H3}$ represent the top and the bottom of the holes (Fig. 4).

## 3. TRANSMISSION DROP FOR PERFECTLY CONDUCTING GRATINGS

### A. Theoretical Demonstration

In this section, our goal is to construct a field that, in some conditions, is the solution of the problem of scattering. Using a time dependence $\exp(-i\omega t)$ and assuming that the incident field is $p$-polarized, an incident magnetic field with unit amplitude, propagating in normal incidence in the upper region (arrow one in Fig. 4), can be written in the form

$$\mathbf{H^i} = H^i\hat{\mathbf{z}} = \exp(-ik_1 y)\hat{\mathbf{z}}, \tag{2}$$

and we deduce from Maxwell's equations the electric field:

$$\mathbf{E^i} = Z_1 \exp(-ik_1 y)\hat{\mathbf{x}}, \qquad Z_1 = \sqrt{\frac{\mu_0}{\nu_1^2\varepsilon_0}} = \frac{Z_0}{\nu_1}, \tag{3}$$

with $\hat{\mathbf{x}}$, $\hat{\mathbf{y}}$, and $\hat{\mathbf{z}}$ being the unit vectors of the axes, $\varepsilon_0$ and $\mu_0$ the permittivity and permeability of vacuum, and $Z_1$ the impedance of the upper region.

We first consider the simplest case where the metallic screen is not perforated by any hole. In that case, the field reflected by the perfectly conducting metallic plane illuminated in normal incidence (arrow 2 in Fig. 4) is given by

$$\mathbf{H^r} = H^r\hat{\mathbf{z}} = \exp(+ik_1 y)\hat{\mathbf{z}}, \tag{4}$$

$$\mathbf{E^r} = -Z_1 \exp(+ik_1 y)\hat{\mathbf{x}}. \tag{5}$$

The total field defined by $\mathbf{E}^\perp = \mathbf{E^i} + \mathbf{E^r}$ and $\mathbf{H}^\perp = \mathbf{H^i} + \mathbf{H^r}$, referred to as the $y$-propagating field in the following, is given by

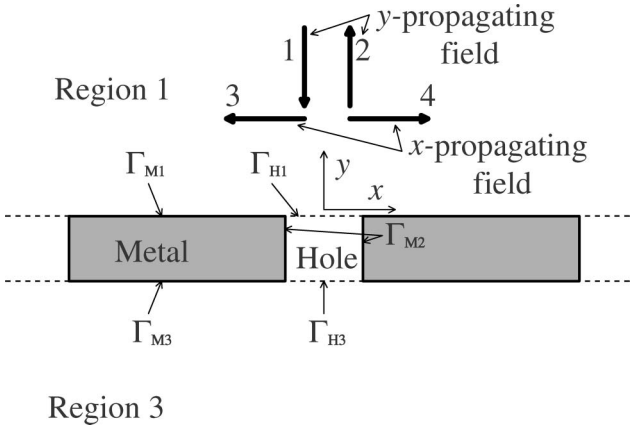


Fig. 4. Interfaces between the different regions and fields of the nonperforated screen. The screen is illuminated in normal incidence by an electromagnetic plane wave of wavelength $\lambda = 2\pi/k$ in vacuum and wavevector $\mathbf{k}_1$ propagating in region 1 (arrow 1 in Fig. 4), thus $|\mathbf{k}_1| = k_1 = \frac{2\pi}{\lambda_1} = \nu_1 k$, $\lambda_1$ being the wavelength in region 1.

$$\mathbf{H}^\perp = 2\cos(k_1 y)\hat{\mathbf{z}}, \tag{6}$$

$$\mathbf{E}^\perp = Z_1[\exp(-ik_1 y) - \exp(+ik_1 y)]\hat{\mathbf{x}} = -2iZ_1 \sin(k_1 y)\hat{\mathbf{x}}. \tag{7}$$

It satisfies the boundary conditions on the plane $y = 0$: the tangential component of the electric field and the normal component of the total magnetic field vanish.

In order to construct the total field in both nonperforated and perforated screen, we introduce a second field $(\mathbf{E}^\parallel, \mathbf{H}^\parallel)$, which we call the $x$-propagating field, corresponding to grazing incidences (arrows 3 and 4 in Fig. 4):

$$\mathbf{H}^\parallel = [\exp(ik_1 x) + \exp(-ik_1 x)]\hat{\mathbf{z}} = 2\cos(k_1 x)\hat{\mathbf{z}}, \tag{8}$$

$$\mathbf{E}^\parallel = Z_1[\exp(ik_1 x) - \exp(-ik_1 x)]\hat{\mathbf{y}} = 2iZ_1 \sin(k_1 x)\hat{\mathbf{y}}. \tag{9}$$

This field is composed of two plane waves propagating in opposite directions along the $x$ axis. As with the $y$-propagating field, the $x$-propagating field $(\mathbf{E}^\parallel, \mathbf{H}^\parallel)$ satisfies the boundary conditions for $y = 0$. It represents the solution of the homogeneous problem (no incident wave) for the nonperforated screen. Thus, according to Eq. (7), all of the components of $\mathbf{E}^\perp$ vanish on the plane $y = 0$, while $\mathbf{E}^\parallel$ is parallel to the $y$ axis, according to Eq. (9). Let us recall that, by definition, the magnetic fields $\mathbf{H}^\perp$ and $\mathbf{H}^\parallel$ are parallel to the $z$ axis.

When the metallic plane is perforated by holes, as shown in Fig. 3, the problem becomes much more complex than a simple problem of reflection by a plane, and it can be expected, in general, that a transmitted field exists. However, $(\mathbf{E}^\perp, \mathbf{H}^\perp)$ and $(\mathbf{E}^\parallel, \mathbf{H}^\parallel)$ still satisfy the boundary conditions on the upper metal interface $\Gamma_{M1}$ of the metallic screen, since this interface has not changed. Moreover, the electric field $\mathbf{E^C}$ of a linear combination $(\mathbf{E^C}, \mathbf{H^C}) = (\mathbf{E}^\perp, \mathbf{H}^\perp) + a(\mathbf{E}^\parallel, \mathbf{H}^\parallel)$, with $a$ complex number, is parallel to the $y$ axis for $y = 0$, while the magnetic field $\mathbf{H^C}$ is parallel to the $z$ axis. Let us suppose that it is possible to find $a$ such that, in addition, the components $H_z^C$ and $E_y^C$ of this combination are equal to zero on the top $\Gamma_{H1}$ of the holes. In that case, all the components of $(\mathbf{E^C}, \mathbf{H^C})$ vanish on $\Gamma_{H1}$. As a consequence, a field that, by hypothesis, is equal to $(\mathbf{E^C}, \mathbf{H^C})$ in region 1 and to zero in the other two dielectric materials will satisfy Maxwell's equations in the entire space and boundary conditions. Indeed, the boundary conditions are satisfied, not only on the top $\Gamma_{M1}$ of the metallic part of the screen but also on the top and bottom $\Gamma_{H1}$ and $\Gamma_{H3}$ of the holes since the electric and magnetic fields vanish on both sides of these boundaries, as well as on the boundaries $\Gamma_{M2}$ and $\Gamma_{M3}$ of the dielectric regions 2 and 3 with the metal since both electric and magnetic fields vanish. Finally, bearing in mind that $(\mathbf{E^i}, \mathbf{H^i})$ is the only incident wave in $(\mathbf{E^C}, \mathbf{H^C})$, and thanks to the theorem of uniqueness of the solution of a problem of scattering, the total field generated by $(\mathbf{E^i}, \mathbf{H^i})$ is equal to $(\mathbf{E^C}, \mathbf{H^C})$. We deduce that the transmitted field will vanish.

The criticism that could be addressed to this demonstration is that the grazing incidence field contains two plane waves propagating parallel to the screen, and, even though they do not bring energy to the grating surface, they can be considered as incident waves in some way. In order to eliminate any doubt, these plane waves will be considered as limits when $\delta \to 0$ ($\delta$ positive) of evanescent waves having a propagation constant along the $x$ axis equal to $k_1 + \delta$ in modulus.

Now, let us show that such a combination of fields can be found, at least approximately. With this aim, we express the $z$ component of the magnetic field and the $y$ components of the electric field at the top of the holes ($y = 0$) using Eqs. (2)–(9):

$$H_z^C = 2(1 + a\cos(k_1 x)), \tag{10}$$

$$E_y^C = 2iZ_1 a\sin(k_1 x). \tag{11}$$

It should be noted that $E_y^c$ vanishes on the $z$ axis, the symmetry axis of the central perforated strip. It can vanish on the symmetry axes of all of the strips provided that $\mathbf{H^C}$ and $\mathbf{E^C}$ have a period $d$ in $x$, which entails that

$$k_1 = pK, \qquad \text{with} \quad K = 2\pi/d, \tag{12}$$

with $p$ being a positive integer. It is worth noting that in the case of Fig. 3, when the perforated screen is a grating, Eq. (12) means that the grazing incidence field is composed of the $(\pm p, 0)$ order [Fig. 3(a)] or the $\pm p$ order [Fig. 3(b)] of the reflected field generated by the normal incidence plane wave contained in $\mathbf{H}^{\perp}$. Thus, this is a case of a Rayleigh anomaly with two passing-off orders [27], which entails that the incident field $\mathbf{H^i}$ included in $\mathbf{H}^{\perp}$ can generate $\mathbf{H}^{\parallel}$.

Obviously, from Eq. (11), $E_y^C$, which vanishes on the sides of the holes, cannot vanish on the entire top of the holes, but it can be close to zero if the width $t$ of the perforated strips is such that $\sin(k_1 t/2) \ll 1$. Thus $k_1 t/2 \ll \pi/2$, which entails

$$t \ll \lambda_1/2 = \lambda/2\nu_1. \tag{13}$$

We deduce from Eqs. (12) and (13) that $t \ll d/2$, and thus the width of the strips must be much smaller than both period $d$ and wavelength $\lambda_1$ in region 1.

Now, we must impose the second condition: the component $H_z^C$ given by Eq. (10) must be small on the perforated strip. To this end, it suffices to impose $a = -1$. In that case, it can be deduced from Eqs. (10) and (13) that $H_z^C$ is very close to zero on the perforated strips and thus is at the top of the holes.

In conclusion, it can be predicted that when the width of the perforated strip (gray region in Fig. 1) is much smaller than both period $d$ and wavelength $\lambda_1$, a strong drop in transmission occurs for a wavelength which, when the structure is a grating, is located close to the passing-off of an order. Furthermore, all of the amplitudes of the reflected and transmitted orders (propagative or evanescent) vanish, except the zero reflected order and the two passing-off orders above the grating. If the integer $p$ of Eq. (12) is greater than 1, this remark entails that all of the reflected and transmitted efficiencies vanish, except that in the reflected zero order, a phenomenon confirmed numerically in Subsection 3.B.

However, let us note that this prediction could fail for discrete values of the parameters of the perforated screen. Indeed, a hole acts like an open cavity. If a resonance of this open cavity occurs, the field inside the cavity could become significant, even though the field is very small on the top of the holes. As a consequence, it could be large inside and below the holes, due to the resonance. Thus the transmission could increase.

Finally, at the first glance, one could think that our conclusion could be deduced from a basic result on waveguides, at least for the 2D grating. It is well known that a perfectly conducting 2D waveguide has a cutoff wavelength and thus cannot transmit light when the wavelength is large with respect to the width of the waveguide. For example, for a circular waveguide, the fundamental mode ($TE_{11}$) has a cutoff wavelength equal to $3.41R$. Such a waveguide cannot transmit light for larger wavelengths. Here, a hole can be considered as a truncated waveguide, and thus it can be conjectured that the transmission by the perforated screen is small. Numerical results will show that this criticism is not relevant. In this regard, let us remark that a truncated waveguide can transmit significant energy by tunneling effect, especially if the thickness $t$ of the screen is not large. It will be shown that the conditions of transmission drop given in this section strongly reduce this tunneling transmission, even for very small screen thicknesses.

Let us note finally that, in our theoretical demonstration of the existence of a drop in transmission, the holes are considered as perturbations of a nonperforated screen. The unperturbed field is $(\mathbf{E^C}, \mathbf{H^C})$, representing a sum of fields in a classical reflection by a plane and fields propagating along the surface of the same plane. The latter fields are the solution of the homogeneous problem, existing at the wavelength given by Eq. (1). We have shown that in some conditions, the unperturbed field vanishes on the upper surface of the holes, and thus it vanishes inside the holes and below the screen. The consequence is that the holes do not create a perturbation of this field or on the wavelength at which it exists.

### B. Numerical Verification: Case of Lamellar Gratings

Figure 5 shows the logarithm of the transmission by a lamellar grating [Fig. 3(b)] as a function of the wavelength. The abscissa represents the factor $\eta$, defined by

$$\lambda_1/d = 1. + 10^{-\eta}. \tag{14}$$

The period of the grating is equal to 1, and thus the $\pm 1$ orders are evanescent and reach the passing-on wavelength when $\eta \to \infty$. The calculations have been performed using the software GRATING 2000, which uses a rigorous integral theory of gratings [32,33]. The transmission (left-hand side of Fig. 3) reaches unity at a wavelength of resonance close to 1.01, then decreases rapidly to a value close to $10^{-7}$ when the wavelength tends to 1. It can be considered that this asymptotic limit is imposed by the limit of precision of the calculations. The modulus of the amplitude $B_{\pm 1}$ of the magnetic field in the $\pm 1$ order above the screen (right-hand side of Fig. 3) tends to unity, after the peak of resonance at $\lambda = 1.01$.

Notice that this asymptotic value is not reached as long as the wavelength differs from $d$ by a value greater than $10^{-5}$. It has been verified that, except for the $\pm 1$ orders, which have a unit amplitude, the asymptotic amplitudes of all other evanescent orders in material one are negligible. The same applies to all of the transmitted evanescent orders. It is not the purpose of the present paper to discuss the peak of resonance (extraordinary transmission) at a wavelength close to 1.01, for which the transmission reaches unity. This result is due to the symmetries of the grating and can be explained using the same arguments as in [34] for the case of dielectric lossless gratings.

Figure 6 shows the same curves as Fig. 5, but with a much greater value of $t$. The phenomenon of resonance holds for the transmission, for a value of the wavelength close to 1.1, which differs much more from the passing-off wavelength than in

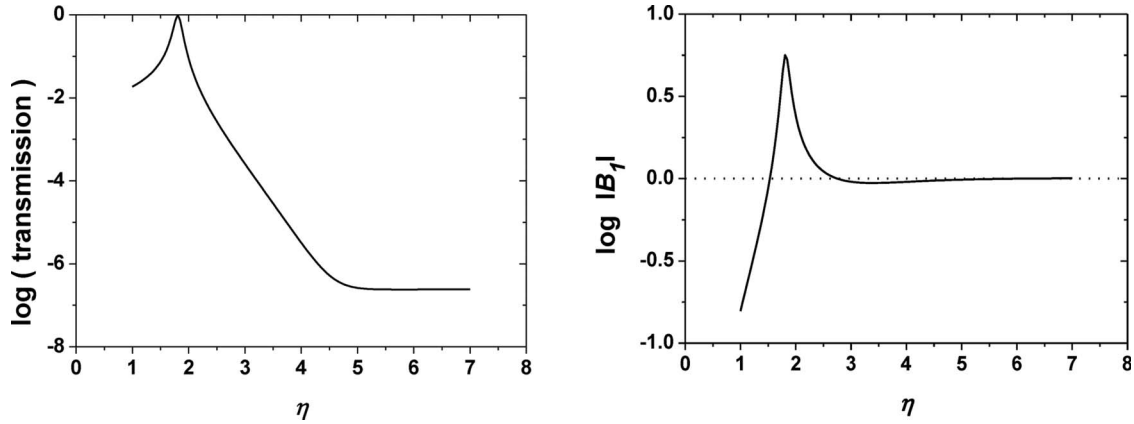


Fig. 5. Decimal logarithm of the transmission (left) and of the modulus of $B_{\pm 1}$ (right) for a perfectly conducting lamellar grating [Fig. 3(b)] having a period $d = 1.$, a width $t$ of the holes equal to 0.05 and a depth $h = 0.3$. The indices $\nu_1$, $\nu_2$ and $\nu_3$ of the dielectric regions are equal to unity.

Fig. 5. The transmission tends to an asymptotic value slightly smaller than 0.1, while the modulus of the amplitude of the first order tends asymptotically to a value close to 1.75. These results are not surprising, since the width of the holes is equal to 60% of the period, and consequently our assumption is not satisfied in that case, but it is worth noting that the transmission tends to a relatively small asymptotic value, as well as the modulus of the amplitude of the magnetic field in the first order.

In order to obtain precise limits of the validity of our theory, in Fig. 7 we show the asymptotic values of the logarithm of the transmission and of the modulus of the amplitude in the first order versus the width $t$ of the holes, keeping the same other parameters as in Figs. 5 and 6. It is very surprising to notice that, even though the limit value of the modulus of the amplitude in the first order rapidly differs from 1 as $t/d$ is increased (it is close to 1.25 for $t/d = 0.35$), the asymptotic value of the transmission remains smaller than $10^{-2}$ as long as $t/d < 0.55$, a value which is much greater than the limit of our basic assumption given by Eq. (13), which states that $t$ should be much smaller than 0.5.

In order to analyze this result, it is interesting to compare the numerical values of the amplitudes and phases of the propagating and evanescent, reflected and transmitted orders on two points of Fig. 7. For $t/d = 0.05$ (left-hand side), the amplitudes of the zero and $\pm 1$ reflected orders are equal to unity and the corresponding phases are equal to 0 (0 order) and 180° ($\pm 1$ orders), as predicted by the theory. The other reflected evanescent orders are negligible (less than $10^{-3}$ in amplitude). The amplitudes of all the transmitted orders are of the order of $10^{-4}$ (including the zero order), except the $\pm 1$ orders, which reach 0.03 in amplitude. For $t/d = 0.5$, the amplitudes of the 0, $\pm 1$, and $\pm 2$ reflected orders are equal to 0.998, 1.48, and 0.185, respectively. The corresponding phases are equal to −14.6° for the 0 order and 172.3° for both $\pm 1$ and $\pm 2$ orders. These values significantly differ from the theoretical predictions, except the amplitude of the 0 reflected order. As regards the transmitted orders, the amplitudes of the 0, $\pm 1$, and $\pm 2$ transmitted orders are equal to, respectively, 0.0557, 0.38, and 0.04. The corresponding phases are equal to 177°, 135°, and 2°, respectively. From these results, it can be deduced that when $t/d$ increases, the phase of the reflected zero order is significantly changed. As a consequence, the boundary conditions on $\Gamma_{M1}$ (metallic part of the top of the screen) are no longer satisfied by the field $(\mathbf{E}^{\mathbf{C}}, \mathbf{H}^{\mathbf{C}}) = (\mathbf{E}^{\perp}, \mathbf{H}^{\perp}) + a(\mathbf{E}^{\parallel}, \mathbf{H}^{\parallel})$. Indeed, although $a(\mathbf{E}^{\parallel}, \mathbf{H}^{\parallel})$ satisfies these boundary conditions for any value of $a$ (it is composed of two plane waves propagating along the $x$ axis), $(\mathbf{E}^{\perp}, \mathbf{H}^{\perp})$ no longer satisfies this condition because the phase of the reflected wave has changed. Thus, evanescent waves of higher orders are needed to fulfill the boundary condition on $\Gamma_{M1}$, which explains the important amplitude (0.185) of the $\pm 2$ reflected orders for $t/d = 0.5$. In the same way, the amplitudes of the $\pm 1$ transmitted orders (0.38 for $t/d = 0.5$ and 0.03 for $t/d = 0.05$) show that the field penetrates inside the holes. However, these orders (which satisfy the boundary conditions on $\Gamma_{M3}$) allow the field that reaches the bottom of the holes to be canceled in such a way that the transmission remains very small. In conclusion,

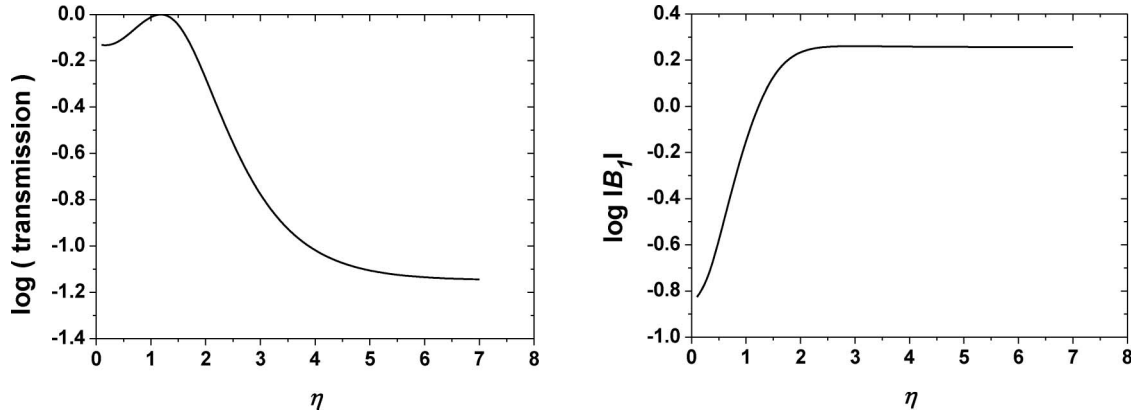


Fig. 6. Same as Fig. 5, but with a hole width $t$ equal to 0.6.

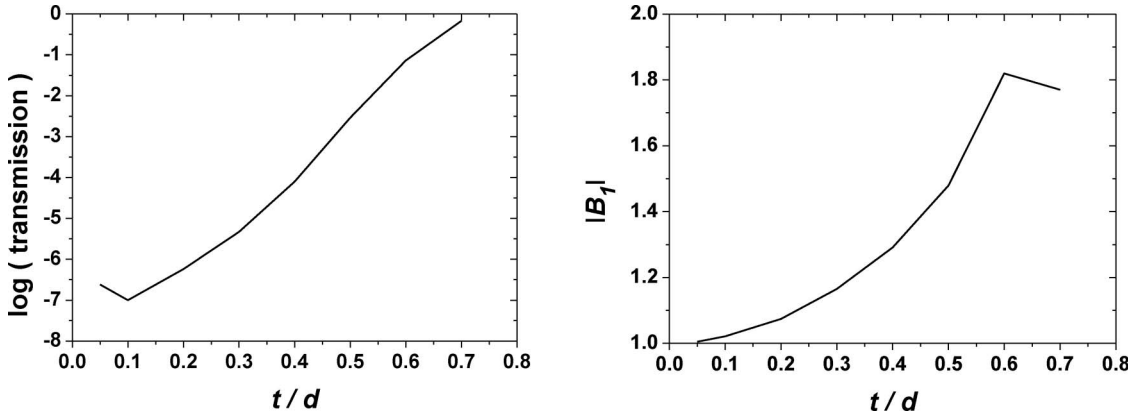


Fig. 7. Asymptotic values when $\eta \to \infty$ of the logarithm of the transmission and of the modulus of the amplitude in the first order with the same other parameters as in Figs. 5 and 6.

the transmission remains small because a complex process involving the 0 (for the phase only), $\pm 1$, and $\pm 2$ reflected orders, as well as the $\pm 1$ transmitted orders, allow the transmitted zero order to remain very small, even though the field can penetrate inside the holes.

Finally, we have analyzed the influence of the width $h$ of the metallic screen. Figure 8 shows the transmission of a lamellar grating having holes of width equal to 0.05 as a function of $h$. The ordinate is the asymptotic value of the transmission as the wavelength tends to 1, with the same parameters as in Fig. 5. The first remark to be made is that the transmission remains very small, even as $h$ decreases. For $h = 0.025$, the transmission does not exceed $10^{-8}$. Problems of convergence occur for smaller values of the screen width. These problems are caused by the integration of Green's functions when the distance between two opposite interfaces of the lamellar grating become much smaller than the wavelength. However, it can be deduced from Fig. 8 that our theoretical demonstration holds for $h \to 0$, the case of a perfectly conducting perforated sheet.

The second important conclusion to be drawn from Fig. 8 is the existence of a peak of transmission around $h/d = 0.6$. This peak can be attributed to a Fabry–Perot resonance of the field inside the hole, which is nothing more than an open cavity. At first glance, it seems that the quality factor of such an open cavity should be poor, since the apertures on both sides of the screen are large. In general, Fig. 8 shows that the transmission of a plane wave inside a hole is very small. By reciprocity, the transmission of the mode on both extremities of a hole also is very small, and this explains why the quality factor is large. The existence of this peak is simply the consequence of the resonant multiple reflections of the mode on these extremities. Bearing in mind that the fundamental mode (which is the unique nonevanescent mode for this wavelength) is constant along the $x$ axis and propagates in $\exp(\pm iky)$ along the $y$ axis, it turns out, assuming a phase shift of the mode at the extremities equal to 0 or $\pi$, that the smallest thickness of the screen that provokes a resonance is equal to $\lambda/2. = 0.5$, which is close to the location of the peak in Fig. 8 (0.5877). Because of the horizontal symmetry of the structure, the transmission peak reaches unity but its width is very small, less than $10^{-4}$.

These remarks show that the phenomenon of transmission drop is confirmed by numerical calculations, except in very small ranges of wavelength where acute resonances occur.

### C. Numerical Verification: Case of Inductive Grids

In order to extend the test of validity to 2D gratings, we next consider the case of a 2D inductive grid [Fig. 3(a)]. The period $d$ along the $x$ axis is equal to unity, as is the period $d'$ along the $z$ axis. Figure 9 shows the variations in the logarithm of the transmission and the logarithm of the modulus $|B_{\pm 1,0}|$ of the amplitudes in the $(\pm 1, 0)$ orders for a small radius. Here, $\pm 1$ and 0 represent the indices $n$ and $m$ of the order, according to the grating formula in normal incidence, giving the components $\alpha_n$ and $\beta_m$ on the $x$ and $z$ axes of the propagation constant in this order:

$$\alpha_n = n\frac{2\pi}{d}, \qquad \beta_m = m\frac{2\pi}{d'}. \tag{15}$$

The passing-off for these orders occurs at a wavelength $\lambda_1$ equal to 1. The transmission remains very small, less than $10^{-8}$, except in the vicinity of $\eta = 4.2$ and $\eta = 6.7$, where it culminates at 100%, and asymptotically tends to 0. The amplitude $|B_{\pm 1,0}|$ tends to unity, as predicted by theory.

Comparing Fig. 9 with Fig. 5, it is evident that the properties of 1D and 2D gratings present some significant differences. First, the transmission and amplitude $|B_{\pm 1,0}|$ includes two peaks in the 2D case (the peak for $\eta = 6.7$ being very acute), while a single one was obtained in the 1D case. The existence of a double peak can be explained very easily. The peaks are

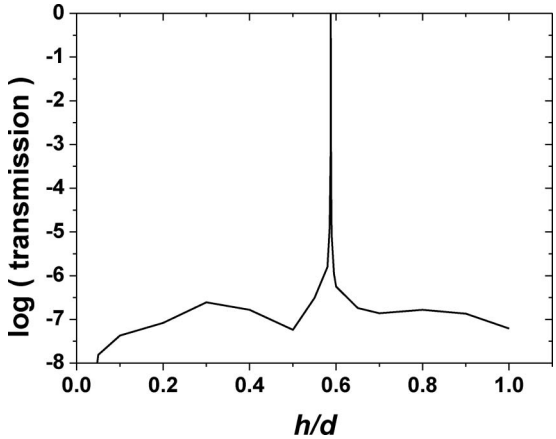


Fig. 8. Variation of the asymptotic value of the transmission of a perfectly conducting lamellar grating as the wavelength tends to one ($\eta \to \infty$), versus the screen depth $h$. The period is equal to 1, the width $t$ of the holes is equal to 0.05. The indices $\nu_1$, $\nu_2$ and $\nu_3$ are equal to unity.

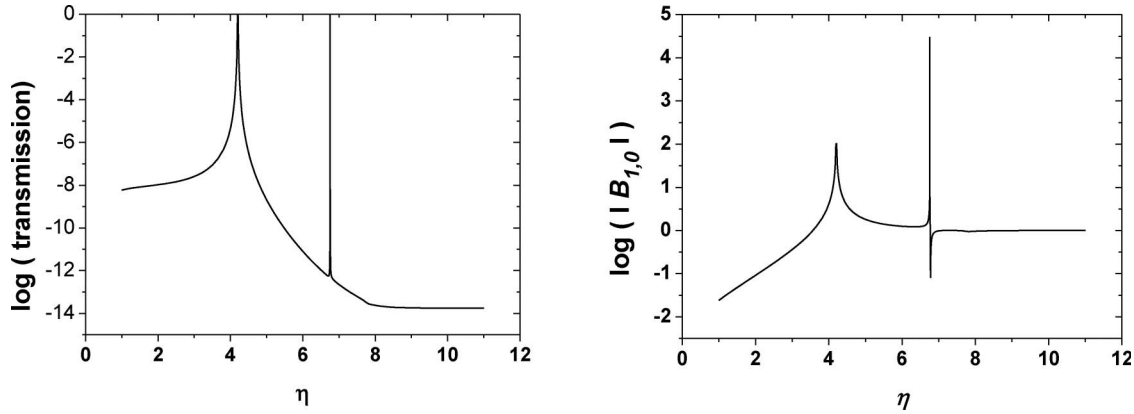


Fig. 9. Decimal logarithm of the transmission and of the modulus of $B_{\pm 1}$ for a perfectly conducting inductive grid [Fig. 3(a)] having periods $d = d' = 1$, with a radius $R$ of the circular holes equal to 0.1 and a depth $h = 0.3$. The indices $\nu_1$, $\nu_2$ and $\nu_3$ are equal to unity.

caused by the excitation of surface waves on both sides of the grating. The horizontal symmetry of the grating entails that two resonances can arise, symmetrical and countersymmetrical. The reason why a single one occurs for 1D gratings is not obvious. It could be linked with the strong difference between the roles of the holes. For a 1D grating, a cutoff wavelength does not exist for the hole that is considered as a waveguide, which entails that a strong coupling exists between the fields on both sides of the screen. This is not so for the inductive grid and, since the wavelength is much greater than the radius of the holes, the coupling between the two sides is much smaller. The shift between the resonance peaks increases with the coupling. It can be conjectured that, due to the strong coupling, one of the resonance wavelengths for the 1D grating is shifted to a wavelength that is smaller than unity and thus cannot appear on the curves.

Figure 10 shows the same curves, but with a greater radius of the holes. As observed for 1D gratings, the asymptotic value of the transmission is strongly increased (from $10^{-14}$ to $10^{-3.5}$) but remains small. On the other hand, the asymptotic limit of $|B_{\pm 1,0}|$ becomes equal to a value close to 2, which is very different than unity, the limit predicted by theory for small holes.

Figure 11 gives the variations of the asymptotic limits of the transmission and $|B_{\pm 1,0}|$ when the radius of the holes is increased. The most striking conclusion to be drawn is that the transmission remains smaller than $10^{-2}$ as long as the radius remains smaller than 0.35, while the asymptotic value of $|B_{\pm 1,0}|$ becomes 40% greater than unity as soon as the radius reaches 0.15, a phenomenon already observed for 1D gratings. The analysis given in Section 3.B for 1D gratings also holds for 2D gratings.

Finally, Fig. 12 shows the logarithm of transmission versus the ratio $h/t$ of the thickness of the screen over the grid period. The oscillations on the left-hand side of the figure are caused by a poor convergence of the numerical results when the thickness of the screen becomes very small, due to a bad integration of the Green's functions. One can observe a quasi-linear variation as soon as $h/t$ exceeds about 0.1. This linear behavior was not observed for 1D gratings. The explanation is straightforward: as mentioned previously, the wavelength is greater than the cutoff value and thus, in contrast with 1D gratings, the transmitted energy is caused by a tunneling effect. This tunneling effect exponentially decreases as $h/t$ is increased, which explains the linear behavior of the logarithm of the transmission. The same explanation can be given for the lack of any resonance peak, compared with the same curves in Fig. 8 for 1D gratings: due to the exponential decrease of the field inside the holes, these holes cannot behave like resonant antennas.

A last remark may be derived from Fig. 12: as observed for 1D gratings, the transmission remains very small (of the order of $10^{-8}$) when the thickness of the screen tends to 0, which shows that our theory applies to the case of a perforated perfectly conducting sheet. From this remark, bearing in mind the Babinet principle, it can be conjectured that complementary properties could be observed for capacitive grids, i.e., structures deduced from the inductive grids by exchanging metal and vacuum inside the grid region: a drop in reflection should

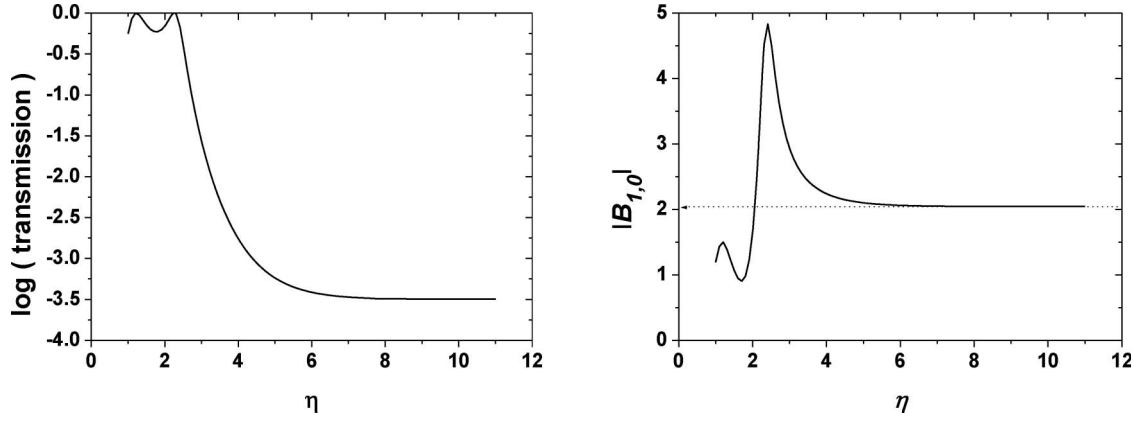


Fig. 10. Same as Fig. 7, but $R = 0.3$.

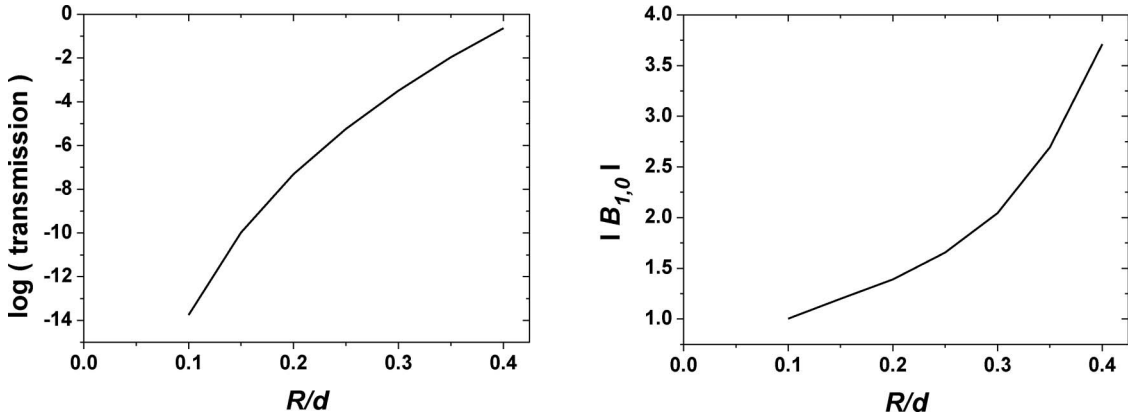


Fig. 11. Variations of the asymptotic values of the logarithm of the transmission and of $|B_{\pm 1,0}|$ with $R/d$. The other parameters are the same as in Fig. 9.

be observed for *s*-polarized light when the radius of the circular metallic elements is small with respect to the wavelength.

In all of the examples given in this paper, the value of the integer $p$ in Eq. (12) is equal to 1: the orders at the passing-off wavelength are the $\pm 1$ orders (1D grating) or $(\pm 1, 0)$ orders (2D gratings). We have verified that if $p$ is greater than 1, all of the reflected and transmitted efficiencies vanish, except that in the reflected zero order. For example, for a 1D lamellar grating with $d = 1$, $t = 0.2$, $h = 0.3$ illuminated in normal incidence by a *p*-polarized plane wave with wavelength 0.2000002, none of the efficiencies of the reflected and transmitted orders exceeds $10^{-3}$, except that of the reflected 0 order, which reaches unity.

## 4. TRANSMISSION DROP FOR FINITE CONDUCTIVITY METALLIC GRATINGS

### A. Theoretical Demonstration

We consider the structure represented in Fig. 3, the metal now having a complex index $\nu_M = (\varepsilon_M)^{1/2}$. The incident electric and magnetic fields are still given by Eqs. (2) and (3). In the simplest case, where the metallic screen is not perforated by any hole and the metal has an infinite extension toward $y = -\infty$, the fields reflected and transmitted by the metallic plane located on the $xz$ plane are given by

$$\mathbf{H^r} = H^r \hat{\mathbf{z}} = \rho \exp(ik_1 y)\hat{\mathbf{z}}, \tag{16}$$

$$\mathbf{E^r} = -\rho Z_1 \exp(ik_1 y)\hat{\mathbf{x}}, \tag{17}$$

$$\mathbf{H^t} = \tau \exp(-ik_{\mathbf{M}} y)\hat{\mathbf{z}}, \qquad k_M = k\nu_M, \tag{18}$$

$$\mathbf{E^t} = Z_M \tau \exp(-ik_M y)\hat{\mathbf{x}}, \qquad Z_M = \sqrt{\frac{\mu_0}{\varepsilon_M}}, \tag{19}$$

with $\rho$ and $\tau$ being the Fresnel coefficients for reflection and transmission by a metallic surface:

$$\rho = (\nu_M - \nu_1)/(\nu_M + \nu_1), \tag{20}$$

$$\tau = 2\nu_M/(\nu_M + \nu_1). \tag{21}$$

Following the same lines as for perfectly conducting metal, we define the *y*-propagating field $(\mathbf{E}^{\perp}, \mathbf{H}^{\perp})$, which is now defined in the entire space by

$$\mathbf{E}^{\perp} = \begin{cases} \mathbf{E^i} + \mathbf{E^r} & \text{for } y > 0 \\ \mathbf{E^t} & \text{for } y < 0 \end{cases},$$
$$\mathbf{H}^{\perp} = \begin{cases} \mathbf{H^i} + \mathbf{H^r} & \text{for } y > 0 \\ \mathbf{H^t} & \text{for } y < 0 \end{cases}. \tag{22}$$

The horizontally propagating fields $(\mathbf{E}^{\parallel}, \mathbf{H}^{\parallel})$ are composed of two surface plasmons [27] propagating in opposite directions along the interface between region 1 and the half-space $y < 0$ filled with metal:

$$\text{for } y > 0, \qquad \mathbf{H}^{\parallel} = \exp[ik(\alpha x + \beta y)] + \exp[ik(-\alpha x + \beta y)]\hat{\mathbf{z}} = 2\cos(k\alpha x)\exp(ik\beta y)\hat{\mathbf{z}}, \tag{23}$$

$$\text{for } y < 0, \qquad \mathbf{H}^{\parallel} = \exp[ik(\alpha x - \gamma y)] + \exp[ik(-\alpha x - \gamma y)]\hat{\mathbf{z}} = 2\cos(k\alpha x)\exp(-ik\gamma y)\hat{\mathbf{z}}, \tag{24}$$

$$\alpha = \frac{\nu_M}{\sqrt{1 + (\nu_M/\nu_1)^2}}, \qquad \beta = \frac{-\nu_1}{\sqrt{1 + (\nu_M/\nu_1)^2}},$$
$$\gamma = \frac{\nu_M^2/\nu_1}{\sqrt{1 + (\nu_M/\nu_1)^2}}. \tag{25}$$

It is important to note that since $\nu_M$ is complex, $\alpha$, $\beta$, and $\gamma$ are also complex. Indeed, due to losses in the metal, the surface plasmon is damped and thus the constant of propagation $k\alpha$ has an imaginary part.

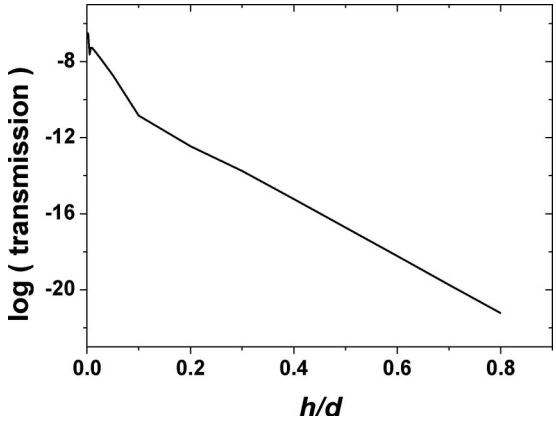


Fig. 12. Variations of the asymptotic values of the logarithm of the transmission with $h/d$. The other parameters are the same as in Fig. 9.

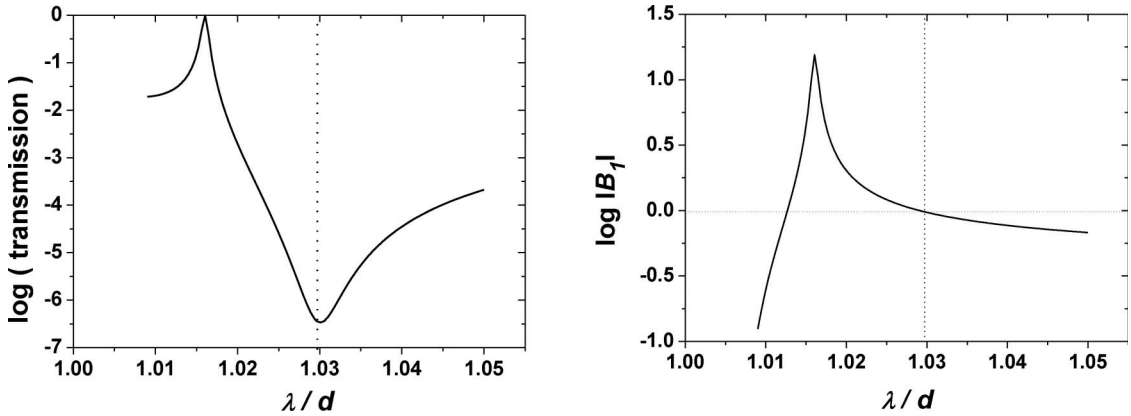


Fig. 13. Decimal logarithm of the transmission (left) and of the modulus of $B_{\pm 1}$ (right) for a metallic lamellar grating with optical index $4.2i$ having a period $d = 1$, a width $t$ of the holes equal to 0.05 and a depth $h = 0.3$. The indices $\nu_1$, $\nu_2$ and $\nu_3$ are equal to unity.

From Eqs. (23) and (24), we deduce using Maxwell's equations:

$$\text{for } y > 0, \qquad \mathbf{E}^{\parallel} = \frac{2Z_1}{\nu_1}[-\beta\cos(k\alpha x)\hat{\mathbf{x}} + i\alpha\sin(k\alpha x)\hat{\mathbf{y}}]\exp(ik\beta y), \tag{26}$$

$$\text{for } y < 0, \qquad \mathbf{E}^{\parallel} = \frac{2Z_M}{\nu_M}[\gamma\cos(k\alpha x)\hat{\mathbf{x}} + i\alpha\sin(k\alpha x)\hat{\mathbf{y}}]\exp(-ik\gamma y). \tag{27}$$

As for the case of perfectly conducting metal, we define a combination $(\mathbf{E}^{\mathbf{C}}, \mathbf{H}^{\mathbf{C}}) = (\mathbf{E}^{\perp}, \mathbf{H}^{\perp}) + a(\mathbf{E}^{\parallel}, \mathbf{H}^{\parallel})$. Thus, the magnetic field $\mathbf{H}^{\mathbf{C}}$ remains, by definition, parallel to the $z$ axis but now the electric field $\mathbf{E}^{\mathbf{C}}$ has nonnull components on both $x$ and $y$ axes

We deal now with the case of perforated screen, shown in Fig. 3. The domain of space including region 1 ($y > 0$) and metal will be denoted by $D_1$ and the complementary region of space by $D_2$. The aim of the demonstration is to show that the field $(\mathbf{E}, \mathbf{H})$ defined by

$$(\mathbf{E}, \mathbf{H}) = \begin{cases} (\mathbf{E}^{\mathbf{C}}, \mathbf{H}^{\mathbf{C}}) & \text{in } D_1 \\ (0, 0) & \text{in } D_2 \end{cases} \tag{28}$$

satisfies, for a given value of the coefficient $a$, Maxwell's equations and boundary conditions between the different materials, at least approximately. Since the only incident wave in that field is $(\mathbf{E}^{\mathbf{i}}, \mathbf{H}^{\mathbf{i}})$, it is deduced that $(\mathbf{E}, \mathbf{H})$ is the total field generated by this incident wave, and thus that the transmitted field vanishes.

The field $(\mathbf{E}, \mathbf{H})$ identifies with $(\mathbf{E}^{\mathbf{C}}, \mathbf{H}^{\mathbf{C}})$ in $D_1$; thus it satisfies Maxwell's equations in this region and boundary conditions (continuity of the tangential components of the fields) on the upper metallic surface $\Gamma_{M1}$ of the screen, which is not changed. If, in addition, the limit in $D_1$ of the $z$ component of $\mathbf{H}^{\mathbf{C}}$ and of the $x$ and $y$ components of $\mathbf{E}^{\mathbf{C}}$ vanish on the boundary of $D_1$ (top $\Gamma_{H1}$ of the holes, vertical sides $\Gamma_{M2}$ of the holes, metallic part $\Gamma_{M3}$ of the lower interface of the screen), then a field equal to $(\mathbf{E}, \mathbf{H})$ will satisfy Maxwell equations in the entire space and boundary conditions on all interfaces between different materials since all the components of the field vanish on both sides of this boundary.

It is very easy to impose $(\mathbf{E}^{\mathbf{C}}, \mathbf{H}^{\mathbf{C}})$ to vanish on the metallic part $\Gamma_{M3}$ of the lower interface of the screen. It suffices to assume that the width $h$ of the screen is much greater than the skin depth $\delta$ of the metal:

$$h \gg \delta. \tag{29}$$

In fact, this condition is not sufficient. At given wavelengths, Fabry–Perot resonances inside the holes can excite surface plasmons at the bottom of the screen, creating an enhancement of the field in this region. Numerical results given in the following (Fig.16) show that this kind of resonance is restricted to extremely small ranges of wavelength.

In order to satisfy the conditions of nullity on the top and on the vertical sides of the holes, we express the field $(\mathbf{E}^{\mathbf{C}}, \mathbf{H}^{\mathbf{C}})$ from Eqs. (2), (3), (16)–(19), and (23)–(27).

On the top $\Gamma_{H1}$ of the holes ($y = 0$),

$$\mathbf{H}^{\mathbf{C}} = [1 + \rho + 2a\cos(k\alpha x)]\hat{\mathbf{z}}, \tag{30}$$

$$\mathbf{E}^{\mathbf{C}} = Z_1\left\{\left[(1-\rho) - \frac{2a\beta}{\nu_1}\cos(k\alpha x)\right]\hat{\mathbf{x}} + \frac{2i\alpha a}{\nu_1}\sin(k\alpha x)\hat{\mathbf{y}}\right\}, \tag{31}$$

and inside the metal

$$\mathbf{H}^{\mathbf{C}} = [\tau\exp(-ik\nu_M y) + 2a\cos(k\alpha x)\exp(-ik\gamma y)]\hat{\mathbf{z}}, \tag{32}$$

$$\mathbf{E}^{\mathbf{C}} = Z_M\{[\tau\exp(-ik\nu_M y) + 2\gamma a\cos(k\alpha x)\exp(-ik\gamma y)/\nu_M]\hat{\mathbf{x}} + 2i\alpha a\sin(k\alpha x)\exp(-ik\gamma y)\hat{\mathbf{y}}/\nu_M\}. \tag{33}$$

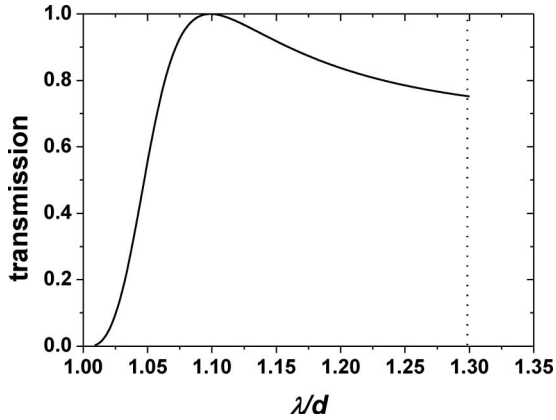


Fig. 14. Same as Fig. 13 (left) but with a width $t$ of the holes equal to 0.6.

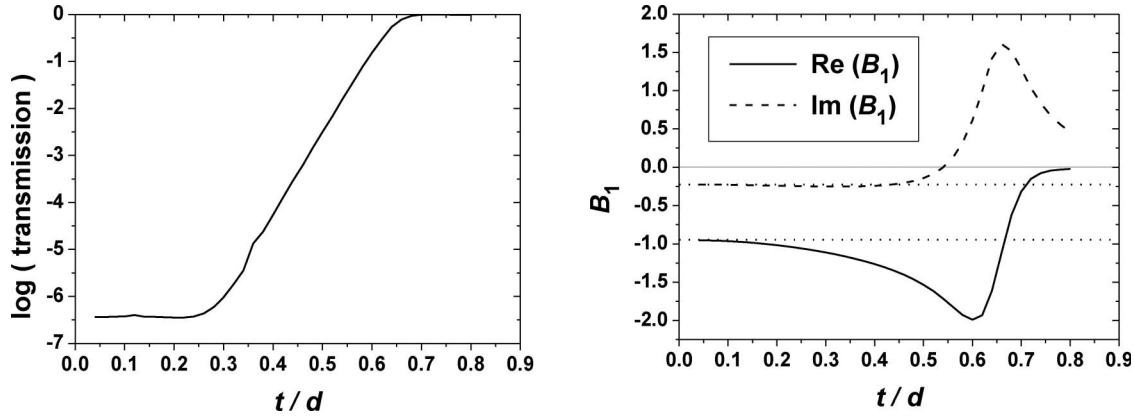


Fig. 15. Values of the logarithm of the transmission and of the amplitude in the first order at the wavelength $\lambda = 1.0296$ given by Eq. (35), keeping the same other parameters as in Figs. 13 and 14. The horizontal dotted lines represent the theoretical values of the real and imaginary parts of $B_{\pm 1}$.

Here, we have to face an initial difficulty. It is possible to impose the magnetic field on the top of the holes, given by Eq. (30) to be very close to zero on the central perforated strip of Fig. 3 (around $x = 0$) by assuming that $t \ll 2\pi/k\alpha$ and taking $1 + \rho + 2a = 0$. However, we must remember that $\alpha$ is complex, and thus $\cos(k\alpha x)$ is not periodic. The consequence is that it is not possible to impose a magnetic field periodic and close to 0 on all the strips of a grating (we exclude here the case where a single strip is perforated). In order to overcome this difficulty, we will assume that the optical index of metal is purely imaginary and greater than $\nu_1$ in modulus. In that case, the permittivity is real and negative, which entails that the conductivity vanishes. As a consequence, there is no Joule effect, the metal becomes lossless, and the constant of propagation $k\alpha$ given by Eq. (25) is real while $k\beta$ and $k\gamma$ are purely imaginary. Since $\cos(k\alpha x)$ is periodic, it is possible to impose the magnetic field $\mathbf{H}^{\mathbf{C}}$ at the top of the holes to be close to 0 on all the perforated strips by setting

$$a = -\frac{1+\rho}{2} = -\frac{\nu_M}{\nu_M + \nu_1}, \tag{34}$$

$$k\alpha = p\frac{2\pi}{d} \Rightarrow \lambda = \frac{d\nu_M}{p\sqrt{1 + (\nu_M/\nu_1)^2}}, \tag{35}$$

$$t \ll 2\pi/k\alpha = \lambda/\alpha. \tag{36}$$

It is worth noting that our assumption about the optical index of the metal is not so unrealistic. For example, at a wavelength of 650 nm, the index of aluminum is equal to $1.3 + i7.1$ and that of silver to $0.07 + i4.2$, and it can be considered that the real part is much smaller than the imaginary part. Also, since $|\nu_M|$ is greater (and even much greater, in many cases) than unity, it turns out that $\sqrt{1 + (\nu_M/\nu_1)^2}$ is imaginary and slightly smaller than $\nu_M/\nu_1$ in modulus. It can be deduced from Eqs. (25), (34), and (35) that $k\alpha$ is slightly greater than $k_1 = k\nu_1$, that $\lambda/\nu_1$ is slightly greater than $d/p$, and that $a$ is complex and close to −1. Furthermore, Eq. (36) can be written as $t \ll \lambda/\nu_1$, which entails from Eq. (35) that $t \ll d$.

In order to simplify Eqs. (30)–(33), we assume that $|\nu_M|^2 \gg \nu_1^2$ (which is the case in the visible, IR, and microwave regions for the usual metals and dielectric materials) in such a way that $\alpha \simeq \nu_1$, $\beta \simeq -\nu_1^2/\nu_M$, $\gamma \simeq \nu_M$, and thus, these equations become, using Eq. (34), on the top of the holes ($y = 0$)

$$\mathbf{H}^{\mathbf{C}} \simeq 2\frac{\nu_M}{\nu_M + \nu_1}[1 - \cos(k\nu_1 x)]\hat{\mathbf{z}}, \tag{37}$$

$$\mathbf{E}^{\mathbf{C}} = 2Z_M\frac{\nu_M}{\nu_M + \nu_1}\left\{[1 - \cos(k\nu_1 x)]\hat{\mathbf{x}} - i\frac{\nu_M}{\nu_1}\sin(k\nu_1 x)\hat{\mathbf{y}}\right\}, \tag{38}$$

and inside the metal

$$\mathbf{H}^{\mathbf{C}} = 2\exp(-ik\nu_M y)\frac{\nu_M}{(\nu_M + \nu_1)}[1 - \cos(k\nu_1 x)]\hat{\mathbf{z}}, \tag{39}$$

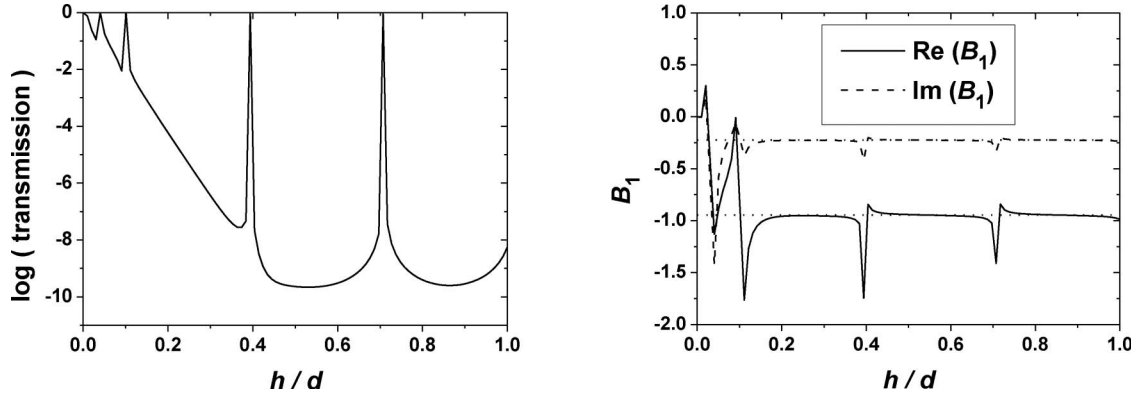


Fig. 16. Variation of the values of the logarithm of the transmission and of the amplitude in the ±1 order at the wavelength $\lambda = 1.0296$, keeping the same other parameters as in Figs. 13 ($t/d = 0.05$). The horizontal dotted lines represent the theoretical values of the real and imaginary parts of $B_{\pm 1}$. The indices $\nu_1$, $\nu_2$ and $\nu_3$ are equal to unity.

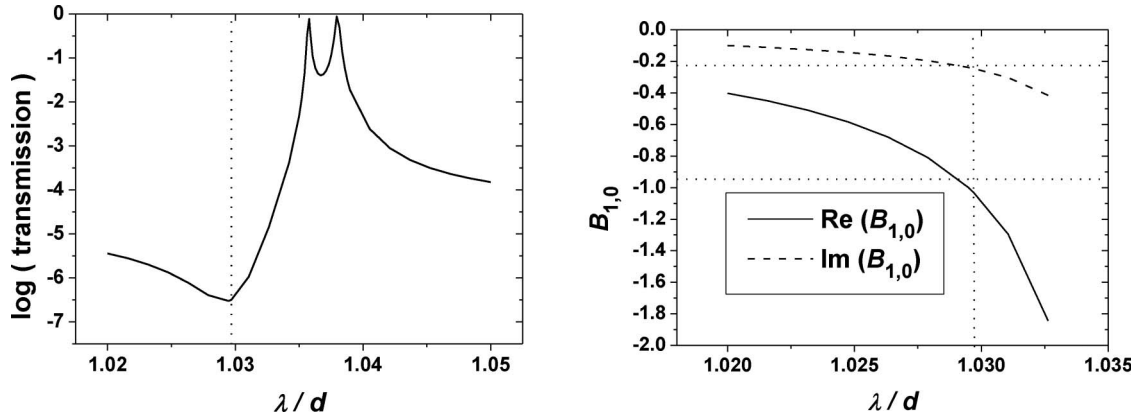


Fig. 17. Values of the logarithm of the transmission and of the amplitude in the first order for a 2D inductive grid with periods $d = d' = 1$, with a radius $R$ of the circular holes equal to 0.2 and a depth $h = 0.3$. The indices $\nu_1$, $\nu_2$ and $\nu_3$ are equal to unity and the index of metal is equal to $4.2i$. The vertical dotted line shows the location (1.0296) of the drop in transmission predicted by theory, the horizontal dotted lines represent the theoretical values of the real and imaginary parts of $B_{\pm 1,0}$ at wavelength 1.0296.

$$\mathbf{E}^{\mathbf{C}} = 2Z_M \exp(-ik\nu_M y)\frac{\nu_M}{(\nu_M+\nu_1)}\left\{[1-\cos(k\nu_1 x)]\hat{\mathbf{x}} - i\frac{\nu_1}{\nu_M}\sin(k\nu_1 x)\hat{\mathbf{y}}\right\}. \quad (40)$$

Bearing in mind that $t \ll \lambda/\nu_1$, it turns out that $\cos(k\nu_1 x) \simeq 1$ on the top of the holes, since $-t/2 < x < t/2$, and that $\sin(k\nu_1 x) \simeq 0$ on the vertical sides of the metal, since $x = \pm t/2$. Thus, all the components of $\mathbf{H}^{\mathbf{C}}$ and $\mathbf{E}^{\mathbf{C}}$ are close to zero at the top of the holes and on their vertical sides provided that Eqs. (34)–(36) are satisfied, and that the thickness of the screen is much larger than the skin depth of the metal. The field generated by an incident field given by Eq. (2) inside the holes and below the screen should be close to zero, except when Fabry–Perot resonances occur inside the holes.

### B. Numerical Verification: Case Of Lamellar Gratings

All calculations on metallic gratings with finite conductivity were performed using the code based on the Fourier modal method, described in Section 2, which can deal with both 1D and 2D gratings.

We first consider the simplest case: the 1D lamellar grating represented in Fig. 3(b). Figure 13 shows the logarithm of the transmission by the lamellar grating as a function of the wavelength. The transmission reaches unity for a wavelength equal to 1.016 but, in contrast to the case of perfect conductivity (Fig. 5), the transmission minimum of $3.4 \times 10^{-7}$ is observed for a wavelength $\lambda = \lambda_1$, close to 1.03. The theory predicts a minimum at a wavelength $\lambda = 1.0296$, given by Eq. (35) (with $p = 1$, since the wavelength and the grating period are close to each other). Thus the agreement between theory and numerical calculations on the location of the drop is excellent. With regard to the amplitude of the first order, the same resonance is observed at a wavelength close to 1.016. In Fig. 17, the vertical dotted lines represent the wavelength 1.0296 of the drop given by the theory, and the horizontal dotted lines represent the theoretical value of $\log|B_{\pm 1}| = \log|a| = -0.0119(|B_{\pm 1}| = 0.973)$ given by Eq. (34). The numerical result is $\log|B_{\pm 1}| = -0.0082(|B_{\pm 1}| = 0.981)$. The corresponding values for the phase of $|B_{\pm 1}|$ are equal to 13.39° for theory and 15.95° for numerical calculations. Thus, the agreement between theory and calculations on $B_1$ can be considered satisfactory. The software based on RCWA cannot handle larger values of the imaginary part of the index, but using the integral theory for an index equal to $7.1i$ (imaginary part of the index of aluminum at 647 nm), a much better agreement (2% in relative value for the modulus and the phase) has been observed.

Figure 14 shows the transmission of the same grating as in Fig. 13, but with a much larger width $t/d = 0.6$ of the holes.

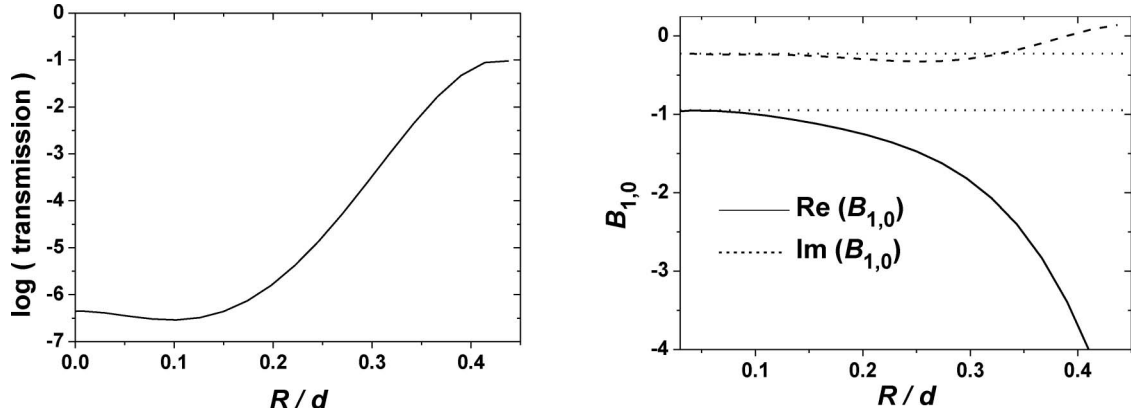


Fig. 18. Variations of the asymptotic values of the logarithm of the transmission and of $B_{\pm 1,0}$ with $R/d$. The other parameters are the same as in Fig. 17.

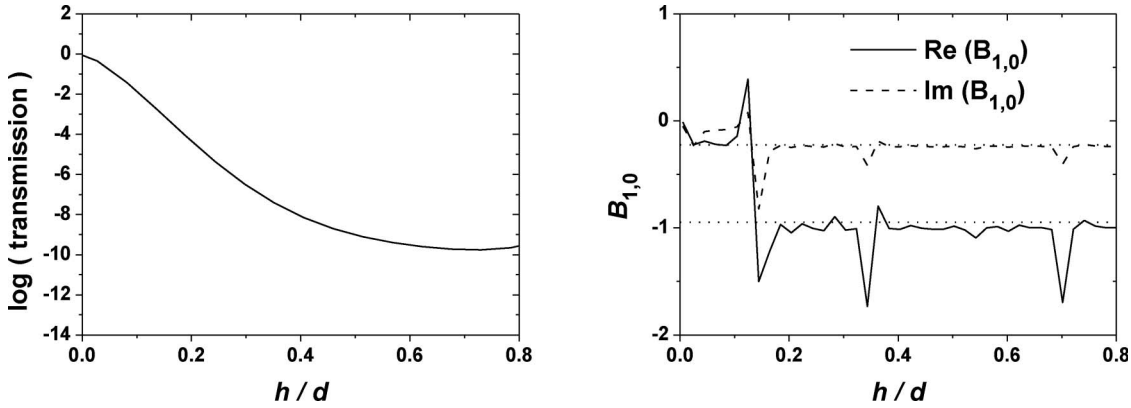


Fig. 19. Variations of the asymptotic values of the logarithm of the transmission and of $B_{\pm 1,0}$ with $h/d$ for $R/d = 0.1$. The other parameters are the same as in Fig. 17.

Obviously, this width is outside the range of validity of our theory: no drop is observed for $\lambda = 1.0296$.

For precision regarding the range of validity of the theoretical predictions, in Fig. 15 we show the values of the logarithm of the transmission and of the real and imaginary parts of the amplitude in the first order versus the width $t$ of the holes, keeping other parameters the same as in Figs. 13 and 14.

As in the case of perfect conductivity (Fig. 7), it is surprising to note that, although the value of $B_{\pm 1}$ significantly differs from the theoretical value as soon as $t/d$ exceeds 0.25, the transmission remains smaller than $10^{-2}$ up to $t/d = 0.53$, which corresponds to a hole width larger than the width of the metal regions. Although the problem for metallic gratings is more complicated, one can conjecture that the bases of the analysis given for 1D perfectly conducting gratings (Sect. 3.B) hold. The agreement between theoretical predictions and numerical results on the limit of $B_{\pm 1}$ as $t$ tends to zero is remarkable.

Figure 16 shows the influence of the metallic screen thickness $h$ on a lamellar grating having hole width equal to 0.05, at the wavelength $\lambda = 1.0296$. In contrast with the case of perfect conductivity, the transmission does not remain very small as $h$ decreases: it exceeds $10^{-2}$ as soon as $h/d$ is smaller than 0.12. This is not surprising if we remember that the width of the metallic screen must be much greater than the skin depth. Here, the skin depth is equal to 0.04, thus we can conclude that the theory remains valid as long as the width of the metallic screen remains larger than three skin depths. This width corresponds to attenuation by a factor close to 20 of a field propagating inside the metal. On the other hand, we observe, as for the case of perfectly conducting metal, some resonances, the most important ones occurring for $h/d = 0.12$, 0.4 and 0.7, with very acute transmission peaks culminating at unity. These resonances create serious discrepancies with theoretical conclusions on the transmission, but on very small intervals of wavelength: for example, the transmission on both sides of the peak at $h/d = 0.7$ falls to a value less than $10^{-7}$ as soon as the thickness of the screen is varied by $10^{-4}$ in relative value. Here again, these peaks can be explained by Fabry–Perot resonances of the field inside the hole.

As for the case of perfect conductivity, it can be concluded that, except in very small wavelength ranges where acute resonances occur, the phenomenon of transmission drop is very robust and extends to a domain that is wider than predicted by theory.

### C. Numerical Verification: Case of Inductive Grids

Figure 17 shows the logarithm of the transmission and of the amplitude $B_{\pm 1,0}$ for an inductive grid with a ratio of radius over period equal to 0.2 and an index $4.2i$. The drop in transmission occurs at a wavelength of 1.0295, very close to the theoretical value, and a double peak of resonance reaches unity at wavelengths close to 1.036. Despite the problems of stability of the calculations and a hole diameter equal to almost half of the grating periods, the agreement between numerical and theoretical results are satisfactory and confirm the validity of the theory.

For precision regarding the domain of validity of the theory, in Fig. 18 we show the curves giving the logarithm of transmission and $B_{\pm 1,0}$ versus $R/d$. Because of numerical instabilities, the curves have been obtained by using a polynomial fit of the data obtained for discrete values of $R/d$. Once again, it must be noticed that, surprisingly, the transmission remains smaller than $10^{-2}$ up to $R/d = 0.35$, i.e., a diameter of 70% of the periods, which obviously is outside the basic hypothesis of the theory. On the other hand, $B_{\pm 1,0}$, which tends to the theoretical prediction when the radius tends to zero, notably differs from the theoretical value as soon as the radius exceeds a value of 0.2. This conclusion is very similar to that stated for the other types of gratings previously studied, and the same analysis (Sect. 3.B) can be given.

In Fig. 19, we represent the variations in the same quantities versus the thickness $h$ of the screen for $R/d = 0.1$. As in the

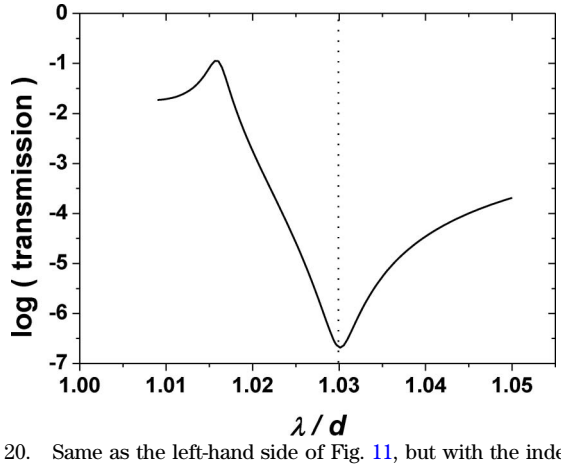


Fig. 20. Same as the left-hand side of Fig. 11, but with the index of silver ($\nu_M = 0.7 + i4.2$) instead of $\nu_M = i4.2$.

case of 1D gratings, the transmission remains smaller than $10^{-2}$ where the width of the screen remains larger than 0.12, i.e., three times the skin depth.

### D. Numerical Verification: Effect of Real Indices of Metals

So far, we have given a purely imaginary value to the metal index. In order to test the validity of our theoretical conclusions for real metals, in Fig. 20 we show the logarithm of the transmission for the 1D lamellar grating of Fig. 13, but with the actual complex index $0.07 + i4.2$ of silver at 650 nm. It turns out that the curve is not significantly modified, except in the vicinity of the peak. This result is not surprising: the peak corresponds to a plasmon resonance, and this resonance generates a strong local enhancement of the field in the metal. In contrast with what occurs for the lossless grating, a large amount of energy is dissipated by Joule effect and thus, the transmission peak in Fig. 20 is reduced by a factor of 10 with respect to the lossless case. However, the location of the drop in transmission as well as the value of the transmission in this region are almost identical.

The conclusion is that the model of lossless metal with a purely imaginary part is accurate, except when a resonance occurs.

## 5. CONCLUSION

The existence of a drop in transmission through hole array has been demonstrated. Assuming that the width of the holes is much smaller than both the wavelength and the grating period, and that the width of the metallic screen is greater than three times the skin depth, it has been shown that this drop is due to the nonresonant propagation of surface plasmons of the nonperforated screen along the surface of the perforated screen. These surface plasmons are generated by the incident wave, and thus the wavelength is given by a very simple equation derived from the grating formula and from the constant of propagation of the surface plasmon on a flat surface. As a consequence, the location of the drop in transmission depends on the metal index only, and not on the shape or width of the holes. It must be emphasized that the drop is not caused by a surface plasmon resonance: the amplitudes of the surface plasmons contained in $\mathbf{H}^{\parallel}$ have the same order of magnitude as those of the incident and reflected fields. In fact, the drop is caused by an antiresonant process that cancels the transmitted field.

Thus, the apparent paradox of this antiresonance phenomenon, which takes place at an alleged resonant excitation of surface plasmons, can be easily explained: the actual resonant excitation of surface plasmons on the surface of the screen arises when the actual surface plasmons of the perforated screen are excited, and the propagation constants of these surface plasmons differ from those of a nonperforated screen.

The phenomenon is quite similar for perfectly conducting screens. In that case, the peak of extraordinary transmission is caused by the resonant excitation of two surface waves propagating in opposite directions along the $x$ axis. These surface waves are nothing more than the limits of surface plasmons propagating on the surface of the perforated screen made of real metal when the conductivity of the metal tends to infinity [27]. In regard to the drop in transmission, it corresponds to the propagation of plane waves with wavevectors parallel to the screen. It can be seen that these plane waves represent a double limit: the limits of surface plasmons of a nonperforated metallic screen as its conductivity tends to infinity, and the limit of the surface waves propagating on a perfectly conducting perforated screen as the radius of the holes tends to 0.

Numerically, it turns out that the domain of existence of the drop is much wider than expected from theory: holes having widths of the order of half a period or half a wavelength are acceptable.

In this paper, we have not given numerical results about nonperiodic structures, especially the very important case of a single hole, where the frequency selectivity of the drop does not hold because the periodicity in $x$ is canceled. This case will be studied in a future paper.

*Note added on proof:* After the paper was accepted, the authors became aware of an earlier related work [35] explaining the zero transmission as a nonresonant superposition of surface plasmons, incident fields, and reflected fields. However, our paper contains a complete, precise, more general theoretical demonstration of the existence of a drop, supported by a wide set of numerical calculations that were not included in the earlier paper.

## ACKNOWLEDGMENTS

The authors thank Philippe Lalanne, who drew their attention to the paradoxical existence of a transmission drop near extraordinary transmission.

## REFERENCES

1. T. W. Ebbesen, H. J. Lezec, H. F. Ghaemi, T. Thio, and P. A. Wolff, "Extraordinary optical transmission through subwavelength hole arrays," Nature **391**, 667–669 (1998).
2. H. F. Ghaemi, T. Thio, D. E. Grupp, T. W. Ebbesen, and H. Z. Lezec, "Surface plasmons enhanced optical transmission through subwavelengths holes," Phys. Rev. B **58**, 6779–6782 (1998).
3. T. Thio, H. F. Ghaemi, H. J. Lezec, P. A. Wolff, and T. W. Ebbesen, "Surface-plasmon enhanced transmission through hole arrays in Cr films," J. Opt. Soc. Am. B **16**, 1743–1748 (1999).
4. T. J. Kim, T. Thio, T. W. Ebbesen, D. E. Grupp, and H. J. Lezec, "Control of optical transmission through metals perforated with subwavelength hole arrays," Opt. Lett. **24**, 256–258 (1999).
5. J. A. Porto, F. T. Garcia-Vidal, and J. B. Pendry, "Transmission resonances on metallic gratings with very narrow slits," Phys. Rev. Lett. **83**, 2845–2848 (1999).
6. E. Popov, M. Nevière, S. Enoch, and R. Reinisch, "Theory of light transmission through subwavelength periodic hole arrays," Phys. Rev. B **62**, 16100–16108 (2000).
7. L. Martin-Moreno, F. J. Garcia-Vidal, H. J. Lezec, K. M. Pellerin, T. Thio, J. B. Pendry, and T. W. Ebbesen, "Theory of extraordinary optical transmission through subwavelength hole arrays," Phys. Rev. Lett. **86**, 1114 (2001).
8. H. J. Lezec, A. Degiron, E. Devaux, R. A. Linke, L. Martin-Moreno, F. J. Garcia-Vidal, and T. W. Ebbesen, "Beaming light from a subwavelength aperture," Science **297**, 820–823 (2002).
9. S. Enoch, E. Popov, M. Nevière, and R. Reinisch, "Enhanced light transmission by hole arrays," J. Opt. A Pure Appl. Opt. **4**, S83–S87 (2002).
10. Q. Cao and P. Lalanne, "Negative role of suface plasmon in the transmission of metallic gratings with very narrow slits," Phys. Rev. Lett. **88**, 057403 (2002).
11. L. Martin-Moreno, F. J. Garcia-Vidal, H. J. Lezec, A. Degiron, and T. W. Ebbesen, "Theory of highly directional emission from a single subwavelength aperture surrounded by surface corrugations," Phys. Rev. Lett. **90**, 167401 (2003).
12. N. Bonod, S. Enoch, L. Li, E. Popov, and M. Nevière, "Resonant optical transmission through thin metallic films with and without holes," Opt. Express **11**, 482–490 (2003).

13. W. L. Barnes, A. Dereux, and T. W. Ebbesen, "Surface plasmon subwavelength optics," Nature **424**, 824–830 (2003).
14. F. I. Baida and D. Van Labeke, "Three-dimensional structures for enhanced transmission through a metallic film: Annular aperture arrays," Phys. Rev. B **67**, 155314 (2003).
15. W. L. Barnes, W. A. Murray, J. Dintinger, E. Devaux, and T. W. Ebbesen, "Surface plasmon polaritons and their role in the enhanced transmission of light through periodic arrays of subwavelength holes in a metal film," Phys. Rev. Lett. **92**, 107401 (2004).
16. E. Popov, M. Nevière, P. Boyer, and N. Bonod, "Light transmission through single apertures," Opt. Commun. **255**, 338–348 (2005).
17. E. Popov, M. Neviere, A. L. Fehrembach, and N. Bonod, "Optimization of plasmon excitation at structured apertures," Appl. Opt. **44**, 6141–6154 (2005).
18. E. Popov, M. Neviere, A. L. Fehrembach, and N. Bonod, "Enhanced light transmission through a circular structured aperture," Appl. Opt. **44**, 6898–6904 (2005).
19. P. Lalanne, J. P. Hugonin, and J. C. Rodier, "Theory of surface plasmon generation at nanoslit apertures," Phys. Rev. Lett. **95**, 902 (2005).
20. K. G. Lee and Q. H. Park, "Coupling of surface plasmon polaritons and light in metallic nanoslits," Phys. Rev. Lett. **95**, 902 (2005).
21. J. Bravo-Abad, A. Degiron, F. Przybilla, C. Genet, F. J. Garcia-Vidal, L. Martin-Moreno, and T. W. Ebbesen, "How light emerges from an illuminated array of subwavelength holes," Nature Phys. **2**, 120–123 (2006).
22. E. Popov, M. Nevière, J. Wenger, P.-F. Lenne, H. Rigneault, P. C. Chaumet, N. Bonod, J. Dintinger, and T. W. Ebbesen, "Field enhancement in single subwavelength apertures," J. Opt. Soc. Am. A **23**, 2342–2348 (2006).
23. C. Genet and T. W. Ebbesen, "Light in tiny holes," Nature **445**, 39–46 (2007).
24. H. Liu and P. Lalanne, "Microscopic theory of the extraordinary optical transmission," Nature **452**, 728–731 (2008).
25. E. Verhagen, L. Kuipers, and A. Polman, "Field enhancement in metallic subwavelength aperture arrays probed by erbium upconversion luminescence," Opt. Express **17**, 14586–14598 (2009).
26. C. Genet, M. P. Van Exter, and J. P. Woerdman, "Fano-type interpretation of red shifts and red tails in hole array transmission spectra," Opt. Commun. **225**, 331–336 (2003).
27. D. Maystre, "General study of grating anomalies from electromagnetic surface modes," *Electromagnetic Surface Modes*, A. D. Boardman, ed. (Wiley, 1982), Chap. 17.
28. L. Li, "Formulation and comparison of two recursive matrix algorithms for modeling layered diffraction gratings," J. Opt. Soc. Am. A **13**, 1024–1035 (1996).
29. L. Li, "New formulation of the Fourier modal method for crossed surface-relief gratings," J. Opt. Soc. Am. A **14**, 2758–2767 (1997).
30. E. Popov and M. Nevière, "Maxwell equations in Fourier space: fast-converging formulation for diffraction by arbitrary shaped, periodic, anisotropic media," J. Opt. Soc. Am. A **18**, 2886–2894 (2001).
31. L. Li, "Use of Fourier series in the analysis of dicontinuous periodic structures," J. Opt. Soc. Am. A **13**, 1870–1876 (1996).
32. D. Maystre, *Diffraction Gratings*, *SPIE Milestones Series* (SPIE, 1993), Vol. MS83.
33. D. Maystre, "Rigorous vector theories of diffraction gratings," *Progress in Optics* 21, E. Wolf, ed. (1984), Chap. 1, 1–67.
34. E. Popov, L. Mashev and D. Maystre, "Theoretical study of the anomalies of coated diffraction gratings," Opt. Acta **33**, 607–619 (1986).
35. P. Lalanne, C. Sauvan, J. P. Hugonin, J. C. Rodier, and P. Chavel, "Perturbative approach for surface plasmon effects on flat interfaces periodically corrugated by subwavelength apertures," Phys. Rev. B **68**, 125404 (2003).